Chapter 3

Site-Controlled Growth of ZnO nanorods and Related Field Emission Properties

3-1 Site-controlled manufacture for FED

The field-emission characteristics of ZnO for both randomly distributed nanowire arrays [162] and single nanotips [163] have been studied recently, and the FE properties of nanostructures are quite similar to those of carbon nanotubes (CNTs). The FE characteristics of ZnO nanowires with various densities have also been discussed. The density of the nanorods critically determines the FE properties. Nanorods of low density generally yield low emitted currents. However, the screening effects of nanorods of high density reduce field enhancement and thus the emitted current. Medium-density nanorods can give a better choice for the emitter density and the interrod distance which is sufficiently large to avoid screening effects. The density and morphology of nanorods must clearly be better controlled for future applications [164]. Hence, the ability to control the growth-site and the density of ZnO nanorods are of interest.

The fabrication of uniformly distributed nanoscale structures has recently attracted much attention. As a nanometer-sized electronic and photonic device, a medium-density and well-aligned nanorod array has great potential for use in fundamental research and practical applications. A general technique for preparing nanorods is by entailing labor upon the desired materials within the pores of a nanoporous membrane [165]-[166] or within the anodic alumina membranes (AAM) with ordered

porous structures [167]. These two approaches can be used to predefine the placement of nanorods by locating metal catalyst islands or particles. However, the distance between the pores and the size of pores in the template still restrict the growth pattern, and the process is not compatible with a standard semiconductor process.

Recently, Li et al. [168] reported the preparation of ZnO nanorod arrays of ZnO by thermally oxidizing the nanorod arrays of Zn. However, those methods need high temperature and a long thermal oxidation process, and synthesizing aligned and well-distributed nanorod arrays of metal oxide at low temperature remains challenging. Synthesis at low temperature not only reduces the heat budget, but also makes the manufacture of the ZnO nanostructures with the microelectronic standard process possible. Besides, if ZnO nanorods are integrated with other electronic devices, the atomic interdiffusion between the deposited layers can be avoided at low temperature. The manufacturing microelectric process is usually conducted under relatively low temperature to reduce the phase transformation of device materials. Therefore, the best temperature for synthesizing nanorods at arbitrary locations in nanodevice integration was below 600 °C. At this temperature, the site-specific nucleation of nanorods must occur, along with a low-temperature growth process that remains site-specific and is compatible with the device platform of interest [169].

Many alternative methods for fabricating nanosized arrays of rods, wires, fibrils and tubules have also been proposed. Huang et al. reported the site-specific nucleation and growth of ZnO nanorods on deposited Au catalyst using a high-temperature vapor transport process [170].

Solution based approaches are the other major technique in fabricating 1-D nanostructures. These processes typically require a

template already molded into the shape of 1-D nanostructure. Filling of the porous template either by solution, sol-gel, or electrochemistry is done to create the desired nanostructure. The advantages of this technique are that it is very versatile and can be used to fabricate various types of 1-D nanostructures as long as the nanostructures are chemically compatible with the template. The nanorods can easily be freed from the template by simply dissolving the template. The biggest disadvantage of this method is that one needs to synthesize the template, which is not a trivial task as it is itself a nanoscaled structure. Fortunately, an anodization process was discovered that transformed aluminum metal into porous aluminum oxide with nanosized channels.

One difficulty in this technique is in ensuring complete filling of the nanochannels as the solution surface tension at the opening of the nanochannels can be extremely high and can impede or block the substances from entering the channel. Li et al. utilized this technique in fabricating ZnO nanorods by first undergoing electrodeposition of Zn creating Zn nanowires in the AAO template, and then subjecting the samples to heat treatments in air to oxide the nanowires [171].

There exists another type of solution based growth process called the solution-liquid-solid (SLS) process. The mechanisms involved in this process are similar to the VLS process except the source is in solution form rather than in vapour form. This solution phase reaction has produced InP, InAs, and GaAs nanowhiskers [172], and more recently, 4 to 5 nm in diameter and several micrometers in length Si nanowires . Up to this point, no known ZnO nanorods have been fabricated using this method.

3-2 Anodized Aluminum Oxide Templates

Anodized aluminum oxide (AAO) templates are composed of varying nanosized diameter channels in a disorder pattern. However, under the right anodization conditions, the AAO can be made to have highly uniform, straight nanochannels in a highly ordered hexagonal pattern.

Fabricating nanostructures and tailoring their properties on the length scales of less than 100 nm by conventional lithographic approaches are quite challenging. In addition, making nanostructures over a large scale (millimeters or centimeters) and into highly ordered, uniform arrays are even more difficult. Such difficulties have compelled many to seek the utilization of recent developments in chemical synthetic methods to produce uniform nanostructures on these length scales, and to form self-organized highly ordered superstructures (i.e. multidimensional superlattices).

The membrane can be used as either the growth template, etch or evaporation mask for the formation of various nanostructures including ZnO nanorods. The alumina nanopore array is formed by anodization of high-purity aluminum under certain carefully controlled anodization conditions. The nanopores can self-organize into a highly ordered array of uniform pores with the pore diameter, the period, and the array size being variable over ranges that are beyond the reach of standard e-beam lithography. As an example, Fig. 14 shows a hexagonally packed template with 55 nm diameter pore sizes spaced 110 nm apart. Each dark area surrounded by the white coloured hexagonal rings is an empty space forming the channels of the template. The channels are perpendicular to the surface and run straight for many microns, depending on the anodization time as shown in Fig. 15.

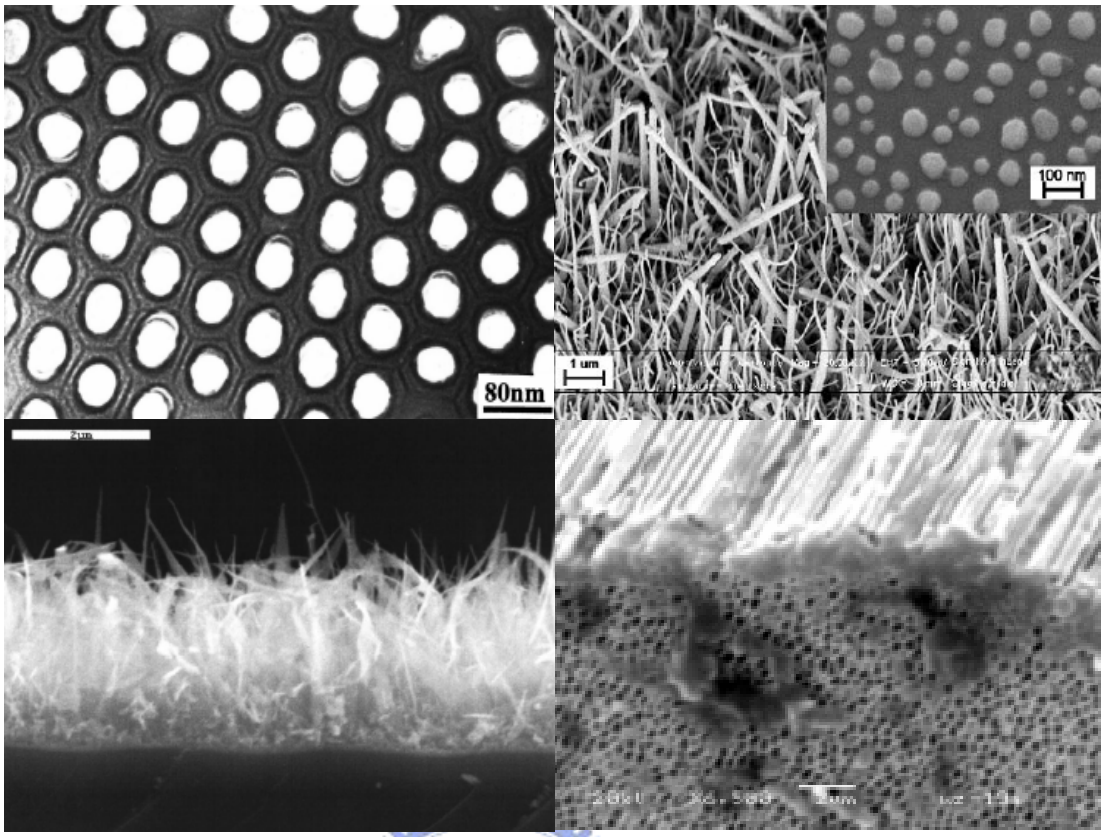

Fig14. SEMimage of the hexagonal, highly order anodized aluminum oxide(AAO) template

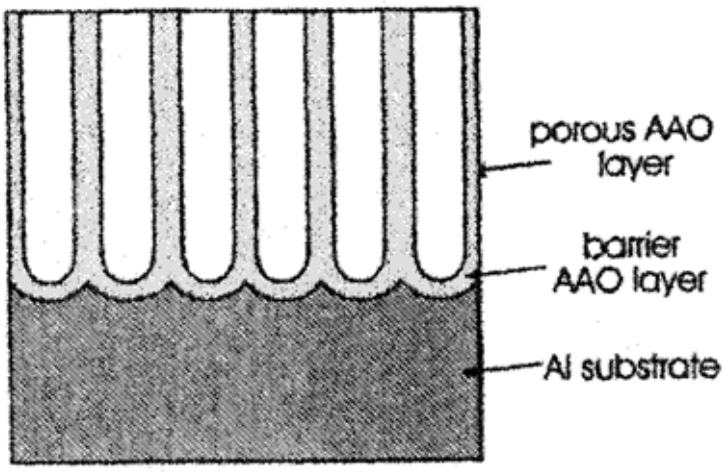

Fig. 15 Schematic illustrating the semi-spherical oxide layer

However, the unique and disadvantageous aspects of the non-lithographic fabrication using self-organized, highly ordered anodized aluminum oxide (AAO) nanopore template include:

- uniform pore diameter adjustable only from 20 nm to 200 nm
- uniform pore periodicity only from 50 nm to 400 nm
- highest but fixed packing density
- the pore diameter, the period, and the array size are not definable
- not compatible with existing IC processing and existing wafer sizes
- Contamination existed

3-3 Standard Semiconductor Process

We have performed the site-specific growth of ZnO nanorods on Si substrate using the submicron semiconductor process under low-temperature conditions. The site-specific substrate was made from a standard VLSI semiconductor process. First, 400nm silicon dioxide was grown on a p-Si substrate by plasma-enhanced chemical vapor deposition (PECVD) at 250 ^{o}C. Second, an array of 0.2 um via holes was generated through submicron lithography and dry etching. Third, a thin Au layer was deposited on the substrate by RF sputtering and then silicon dioxide was partly removed by the lift-off process. Consequently, an Au catalyst, with or without , was depsoited on the flat surface of every hole predefined by residual silicon dioxide. The process flow was shown in Fig. 16.

According to the growth mechanism discussed in chapter 2, ZnO nanorods might easy locate at the hillock and etchpit. After the lift-off process of silicon oxide, there were many etchpits for Zn vapor to condense to form the site-controlled ZnO nanorods.

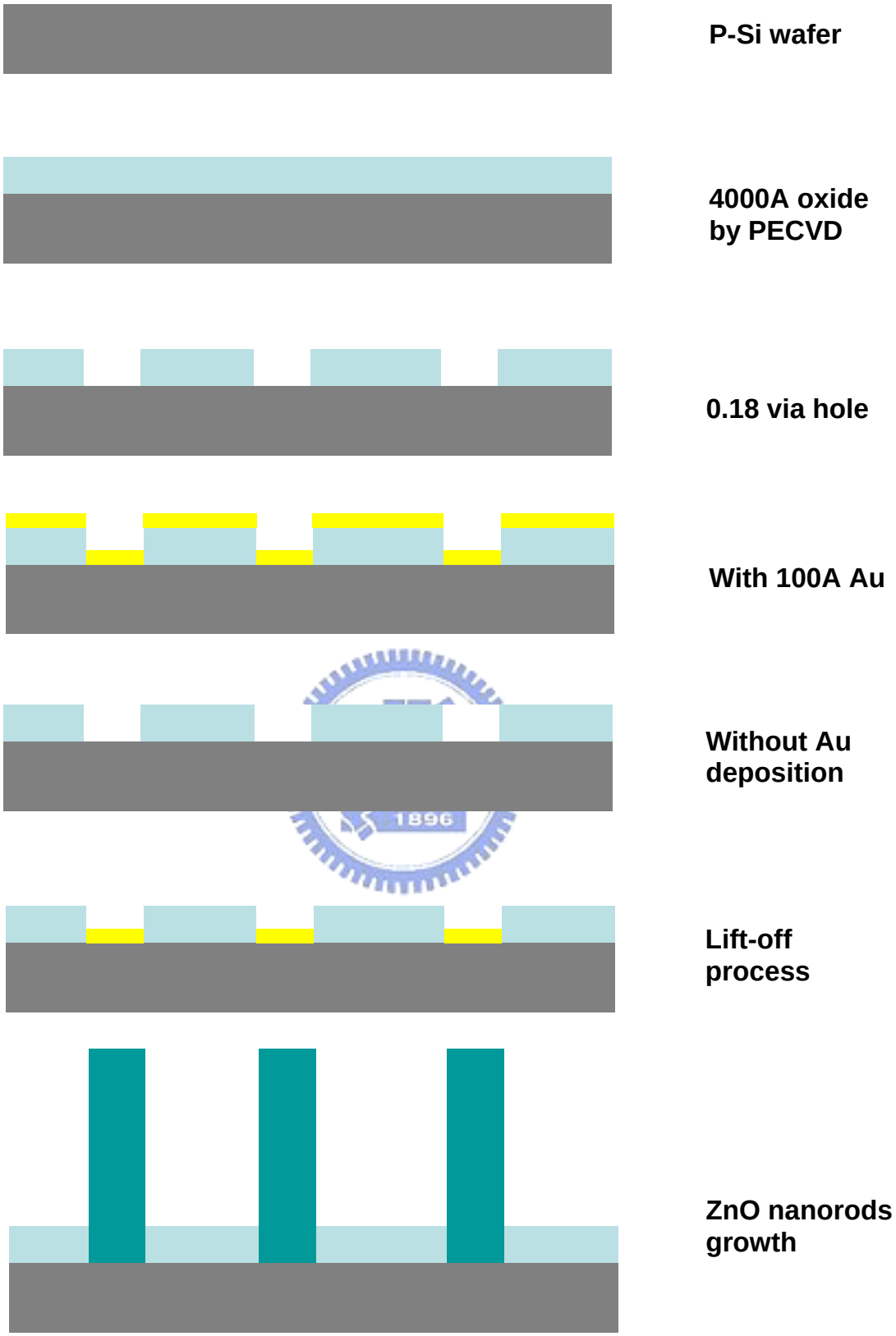

Fig. 16 Standard semiconductor process flow

The ZnO nanostructures were fabricated from Zn powder on the prepared patterning substrate by a thermal evaporation process in vacuum. The synthesis was carried out in a quartz tube with Zn powders as the source material. The quartz tube was then put into a horizontal furnace. The temperature was set to 600 ^{o}C and the carrier gas, Ar, flowed inside the quartz tube for two hours.

The material properties were investigated by FESEM, EDX, XRD and PL. Large area FE measurements were made using two-parallel-plate configuration in a vacuum chamber as shown in Fig. 17. The cathode made by patterned nanorods of ZnO remained 100μm away from the anode which is a glass plate with phosphor coated. As for the local FE properties, the anode was changed to a tip with radius of 600 μm to measure the different areas of different densities in the same sample. The emission current was measured by applying an increasing voltage from 1V to 900V, in sweep steps of 10V, and was measured using a Keithley 237 I-V meter.

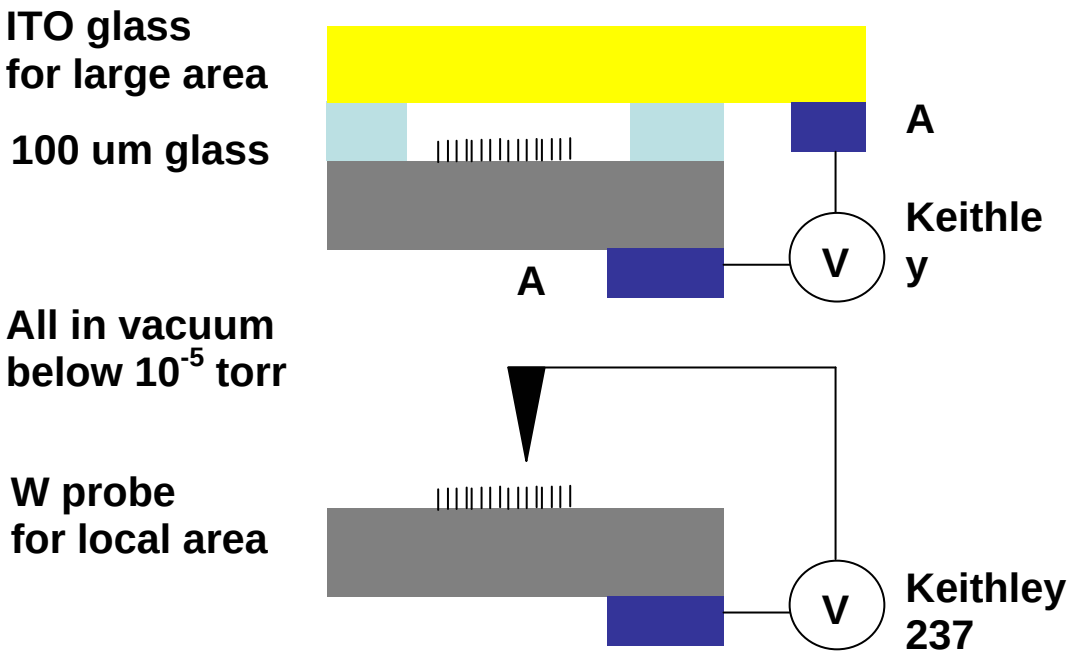

Fig. 17 Field emission experiment for large and local area

3-4 Field Emission Properties of Patterned ZnO Nanowire and Mechanism Discussion

Figure 18(a) display Images of the site-specific growth of ZnO nanorods obtained by FESEM. Arrayed ZnO nanorods were grown from each 0.2um via hole. A wetting layer under these nanorods was found inside each hole, and the direction of the nanorods was changed according to the morphologies of that wetting layer. After decreasing the carrier gas, the number of ZnO nanorods in every hole was reduced. As shown in the more highly magnified image of Fig. 18(b) and Fig. 18(c), a single nanorod was formed in a hole and its appearance was changed from hexagonal prismatic at the top to cylindrical at the base. The average diameter and length of these nanorods were about 100~200nm and ~1 um, respectively.

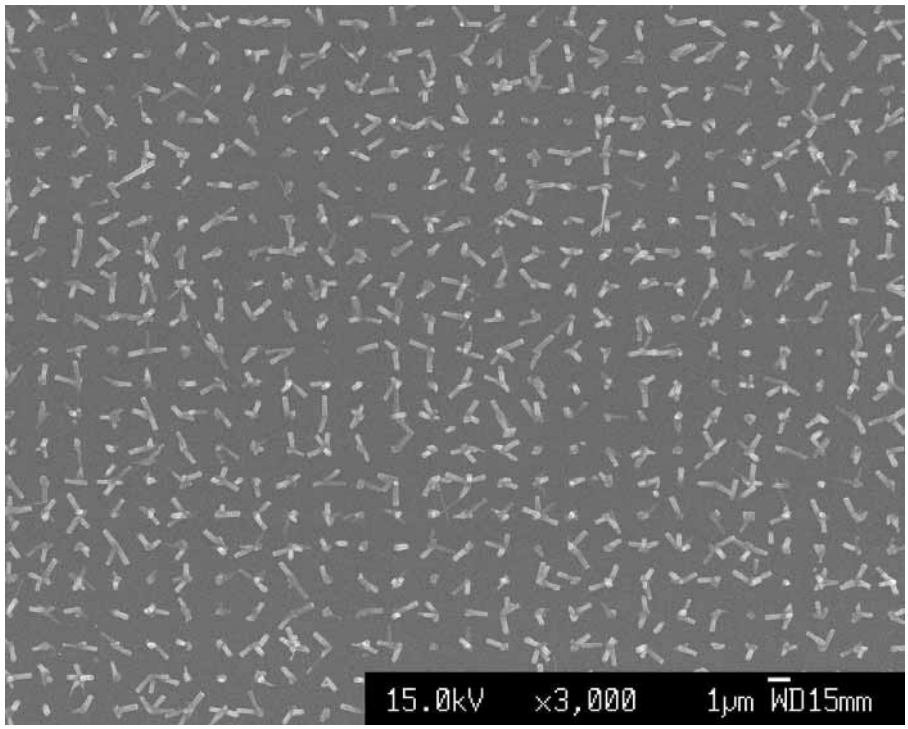

Fig. 18. (a) patterning growth of ZnO nanorods formed from each 0.2um via hole.

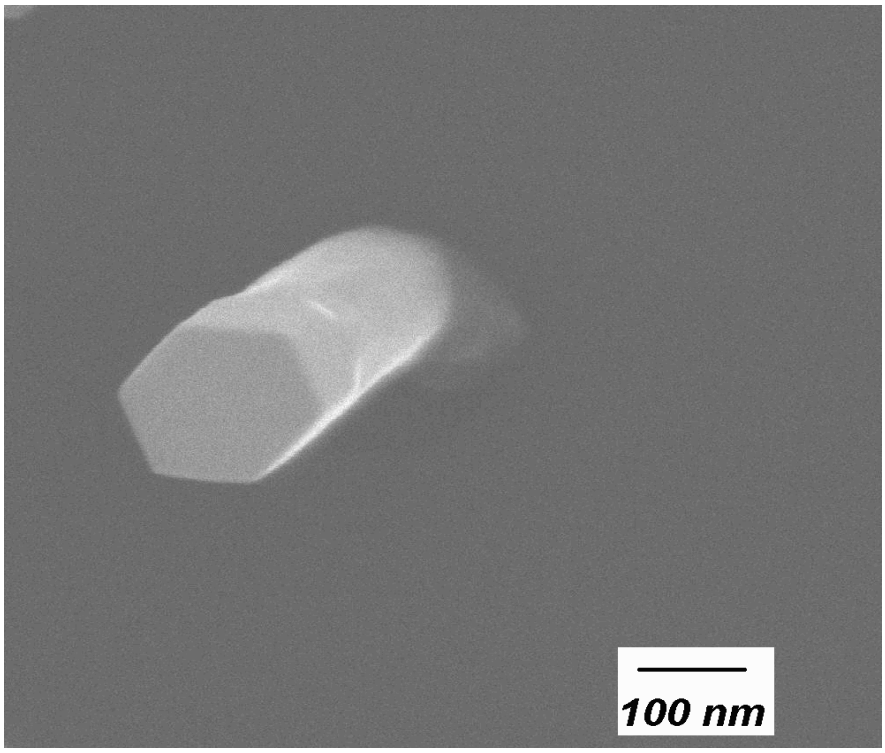

Fig.18. (b) prismatic structure at the top part and cylindrical shape at the base part of the single ZnO nanorod.

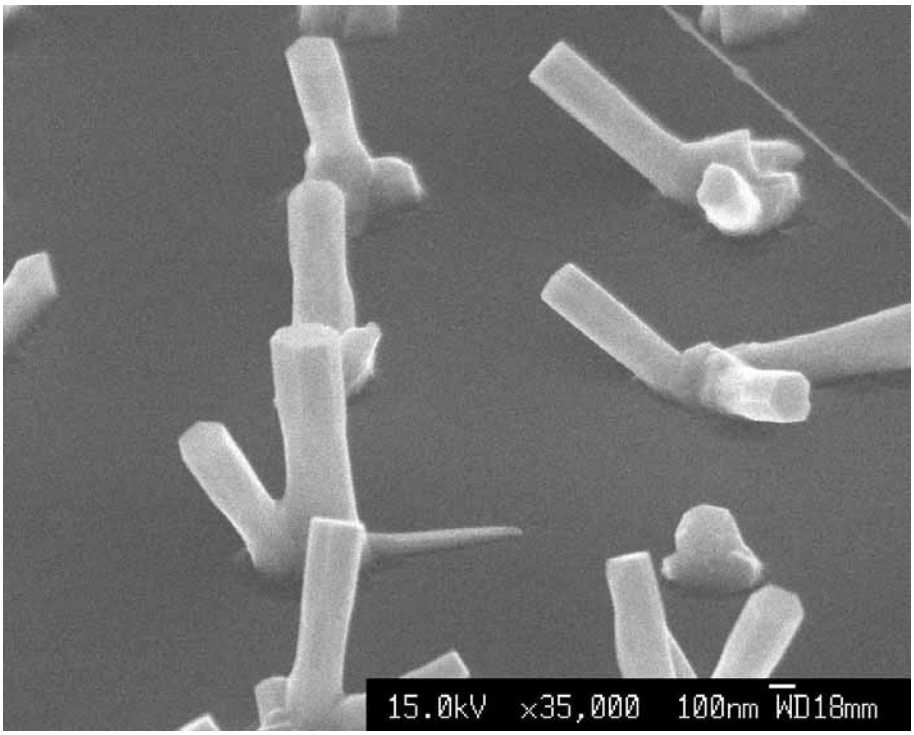

Fig.18. (c) tilt angle image of site-specific ZnO nanorod.

Figure 19(a) shows the structure of the site-specific growth of ZnO nanorods. The XRD pattern indicates that the peak positions of XRD were consistent with those of the hexagonal structure of bulk ZnO with lattice constants of ao=3.32489Å and co=5.2062Å. The sharp peak and the specific strong (002) peak demonstrates that the nanorods had a good wurtzite structure and grew along the prefer orientation of [001]. EDX analysis also indicates that the nanorods consist only of ZnO. Fig. 19(b) presents the PL spectrum. The main emitting bands observed from the PL spectrum of ZnO nanorods at room temperature is a strong ultraviolet (UV) emission at around 380nm, and is accompanied by a weak green emission near 500nm. A strong UV peak associated with near band edge emission is present because of the good crystalline quality of ZnO. Weak green emission is also known and indicated that the nanorod includes some singly ionized oxygen vacancies [173].

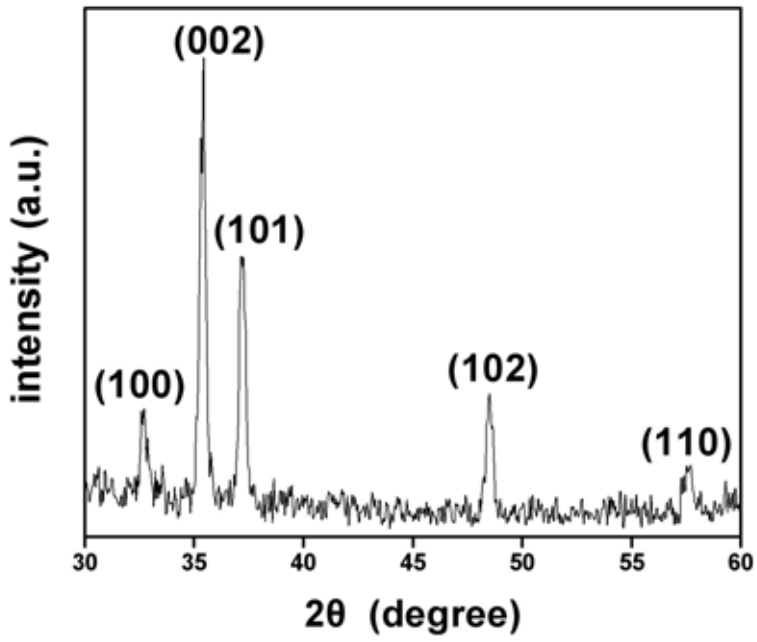

Fig. 19(a). XRD pattern of site-specific ZnO nanorods. The sharp peak from (002) indicate good crystallinity

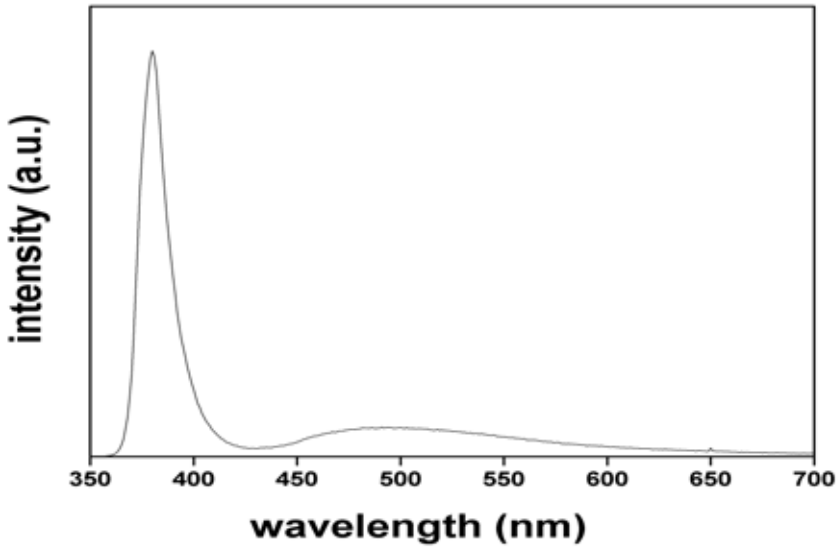

Fig. 19(b). PL spectra of site-controlled ZnO nanorods

The nanorod undergoes a growth mechanism through the Au catalyst. Accordingly, the highly concentrated Zn vapor can initially condense easily on the central flat surface of every patterned hole. Some droplets of Zn-Au alloy then acted as new nucleus sites for growing nanorods because the surfaces of the droplets had a high sticking coefficient and therefore become preferred sites for absorbing zinc vapor [174]. The catalyst critically determines the rod diameter, when the super saturation from the vapor is appropriately controlled. However, each patterned hole can also provide an anisotropic surface near the edge. The anisotropic surface can generally affect the growth in two features. First, it can induce anisotropic strain, confining the diffusion of adatoms. Second, it generates two nucleation sites to produce nanorods - nanoscale etched pits and hillocks [175]. Consequently, vapors of Zn and Zn suboxides were condensed not only on the centered flat surface of the hole, due to the catalyst, but also on the anisotropic surface from the sidewall of the hole. During growth, a wetting layer with polycrystalline structure formed

gradually in the hole. As the ZnO rods lengthened, they grew quickly from the polycrystal to the [001] direction, forming a flat plane, thereby reducing the surface energy. Thus, the other facets of the ZnO nanorods gradually disappeared [176]. However, by with this technique, no ZnO nanorod can be controlled to grow vertically toward the substrate since the roughness of the surface is such that nanorod can be formed at any possible angle on the polycrystalline wetting layer. As the concentration of Zn decreased during the growth process, the well-wurtzite structure was gradually formed with the oxygen provided by residual oxygen gas. The process could be tuned to make all rods grow in the same direction such that each site contains only one nanorod.

Figure 20 illustrates the field emission property of a site-specific growth of ZnO nanorod array grown on the p-Si substrate. The emission current-voltage characteristics were analyzed using the following Fowler–Nordheim (FN) equation;

$$J=A(\beta^2V^2/\Phi d^2)\exp(-B\Phi^{3/2}d/\beta V) \quad (2)$$

where J is the current density; A=1.56×10-10 (AV^{-2} eV); B=6.83×109 ($VeV^{-3/2}$ Vm^{-1}); β is a field enhancement factor; Φ is the work function; E=(V/d) is the applied field; d is the distance between the anode and the cathode, and V is the applied voltage [177]. The turn-on voltage, which is defined as the field where the emission current density can be districted from the background noise [178], was approximately 6.0 V/μm at a current density of 0.05 mA/cm^2. The emission current density reached about 0.33 mA/cm^2 at an applied field of about 8.0 V/ μm (the so-called threshold field) [162]. Both the turn-on and the threshold voltage were comparable to those of CNTs. Smaller or more sharply tipped nanorods, and a lower areal density of the nanorods yielded better FE properties [164]. The emission current

from ZnO nanorods produced sufficient brightness for flat panel displays [177]. Figure 15 also presents the FN logarithmic plot, which exhibits linear behavior over the measurement range, so the emission is indeed caused by the F-N tunneling mechanism.

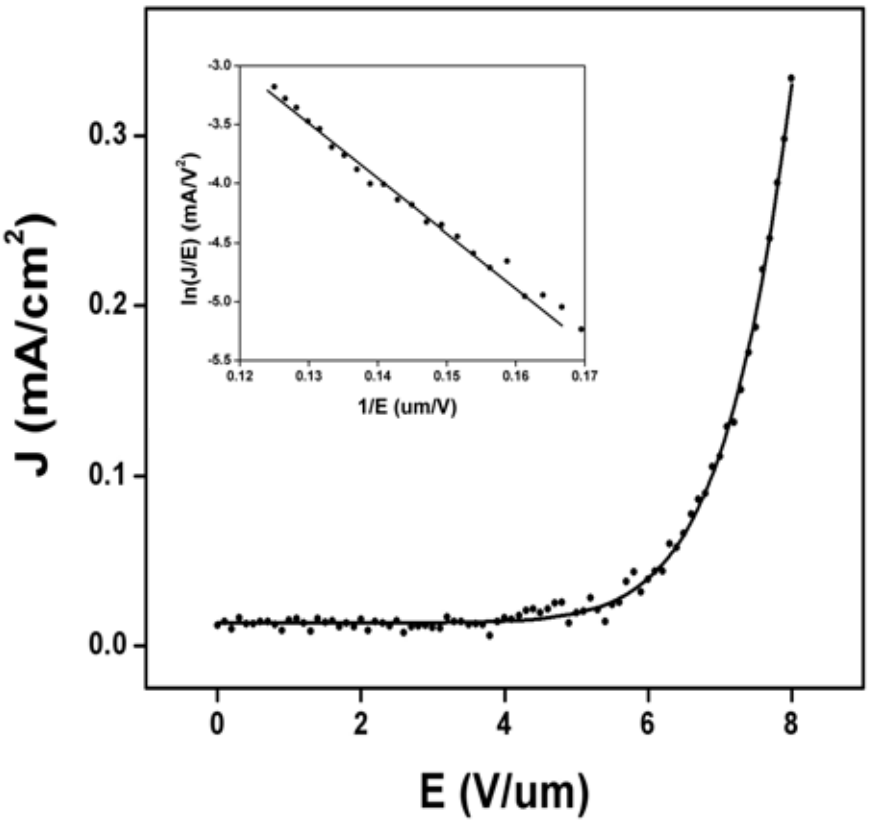

Fig. 20. The field emission I-V curves from the patterned ZnO nanorod array. The turn-on voltage was about 6.0 V/μm at current density of 0.05 mA/cm^2. The inset depicted F-N logarithmic plot, which satisfied the F-N tunneling mechanism by exhibiting a linear behavior over a measurement range.

Figure 21 display images of the dense ZnO nanorods obtained by FESEM. The directions of those cylindrical nanorods were randomly arranged at the predefine region and their average diameter and length were about 70~100nm and 2~3 um, respectively. According to the X-ray data, those nanorods were ZnO with very good crystalline structure. Every single nanowire was crystalline with hexagonal prismatic appearance as shown in the more highly magnified image of Fig. 16

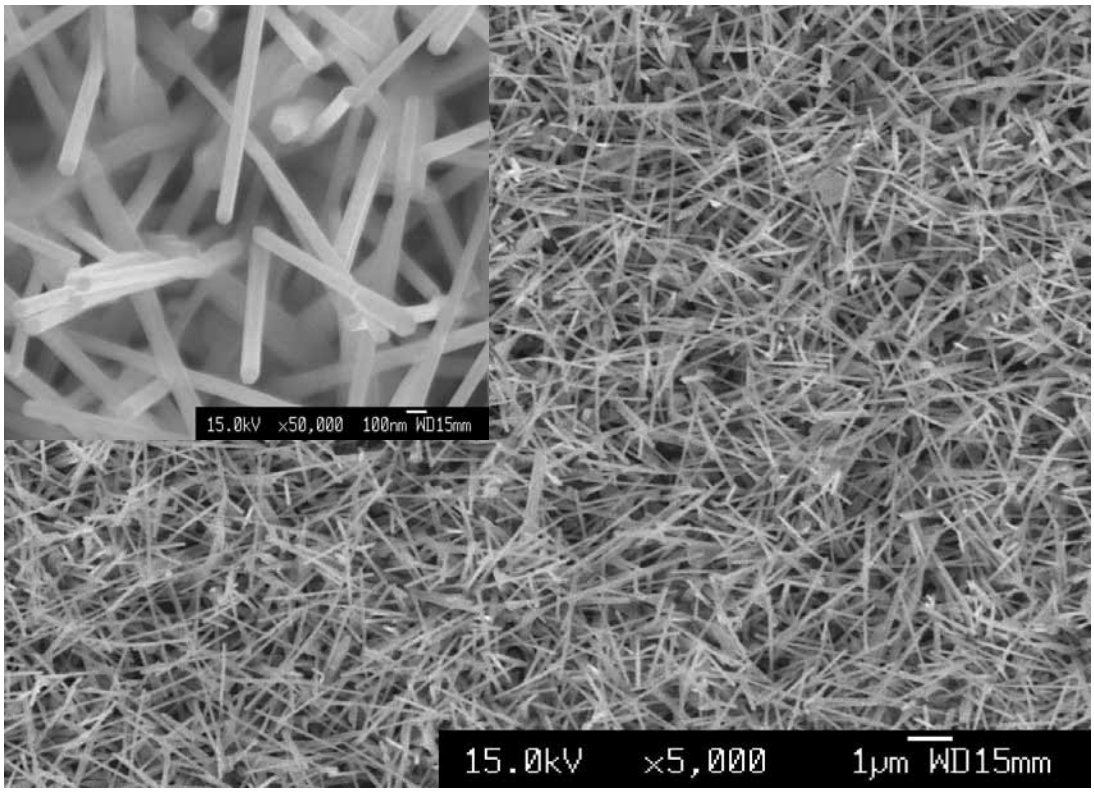

Fig. 21. FESEM image of ZnO nanorods and their average diameter and length were about 70~100nm and 2~3 um, respectively. The inset depicted the more highly magnified image, which exhibited a prismatic crystalline structure of the single ZnO nanorod.

The local FE properties of different nanorods densities were shown in Fig. 22 and the average turn-on fields (~8 and 14 V/μm) were comparatively larger than that of the integrated FE property. The reason will be explained as follows. The integrated emission was dominated by a comparatively small number of very strong emitting sites spread out over the entire sample surface. Indeed, the number of detectable emission sites depends on the area of the measured surface. One cm^2 area will include more strong emitting sites, than a local measurement in one mm^2 window, hence a higher field enhancement factor (β) and a lower turn-on field is expected for integrated FE emission.

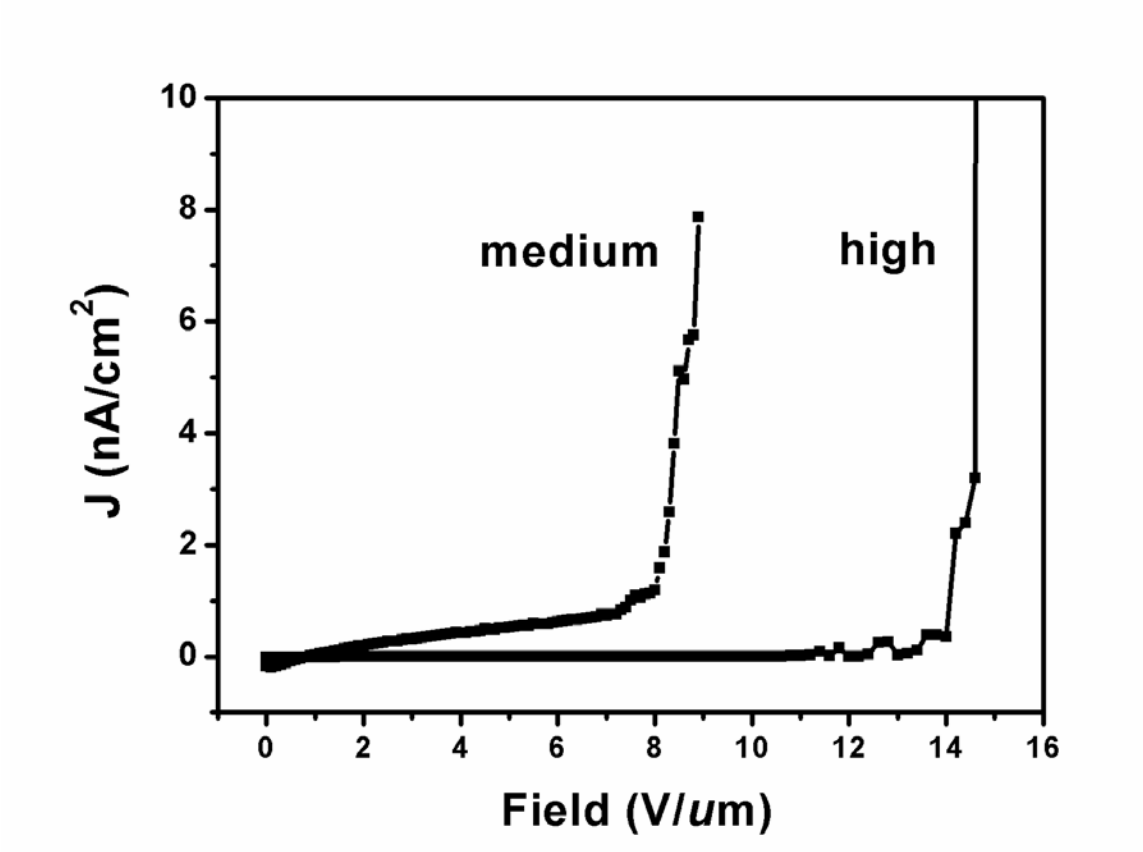

Fig. 22 FE properties of different nanorods densities and the average turn-on fields (~8 and 14 V/μm) were shown.

The poor emission of higher density nanorods is explained by an electrostatic screening effect provoked by the proximity of neighboring

rods shown in Fig. 23. The solution of the Poisson equation governs the behavior of the potential between the nearby ZnO deposit, hence β depends on the inter distance of nanorods (**l**). The β values, calculated from the FN logarithmic plot, of high and medium density of ZnO nanorods are 443 and 735 respectively. A function about film f(l) = 1-exp(-1.1586l) that characterizes the decrease in the field amplification due to inter-rode screening [179]. Since it is the local electric field at the emission site that governs the emission, the distance between the nanorods remains a crucial parameter to optimize the FE. For the medium density, there is an ideal compromise between the emission current and the β factor, which shows a better FE performance.

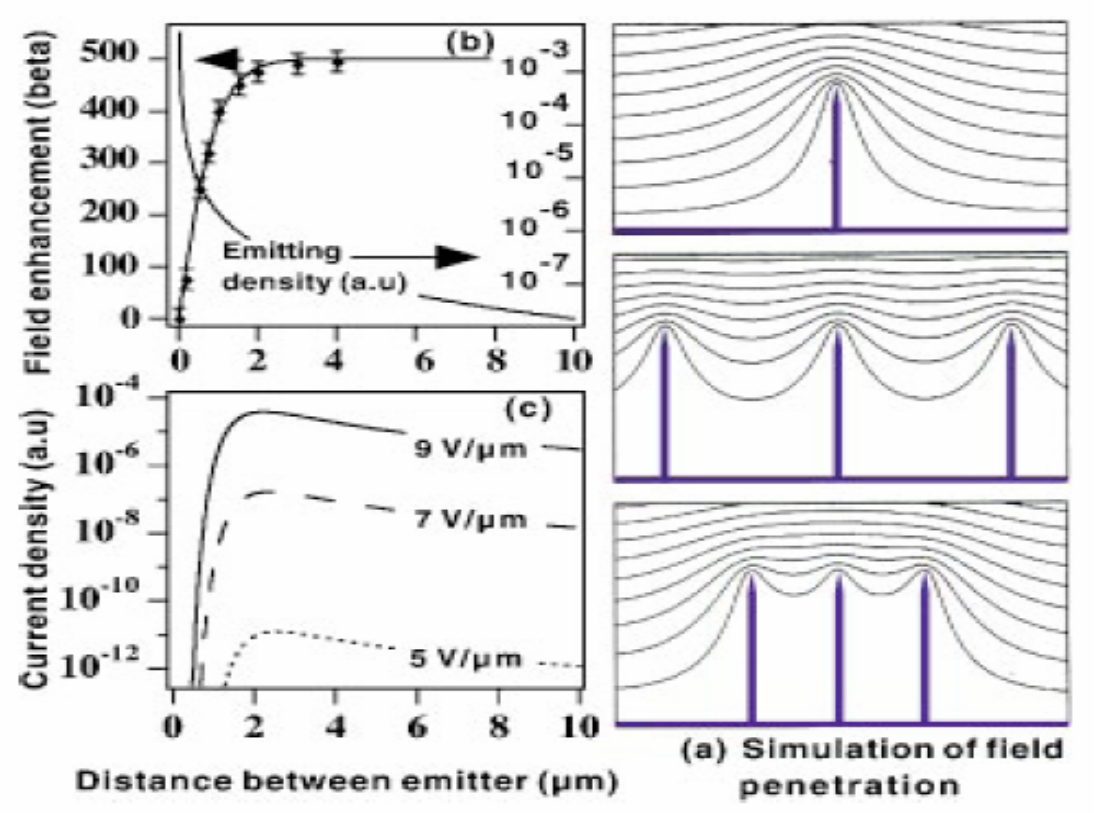

FIG. 23. (a) Screen effect simulation of the equipotential lines of the electrostatic field along with the corresponding changes of the field enhancement factor band emitter density (b), and current density (c) as a function of the distance.[180]

3-5 Conclusion

Site-specific nanorods of ZnO were successfully grown on silicon substrate with PECVD and standard submicron lithography process operated at low temperature. The selective growth of ZnO nanorods at a relatively low growth temperature suggests that it can be integrated on device platforms for nanoelectronics. In addition, this technique also gives advantages of controlling the growth site and varying the proper interrod distance as well as the emitter density while growing the ZnO nanorods.

A field emission experiment for such patterned ZnO nanorods was conducted to indicate the F-N tunneling model. Sample of medium density (~25#/um^2) is shown a better field enhancement factor than that of higher density (~375#/um^2). Therefore, uniformly distributed the nanorods with a medium density by site-specific growth is thus clearly required and this approach was demonstrated the possibility of the integration of FE nanodevices by one-dimensional ZnO nanorods on a silicon substrate.